periodica polytechnica

Civil Engineering
57/1 (2013) 45–61
doi: 10.3311/PPci.2141
http://periodicapolytechnica.org/ci
Creative Commons Attribution

RESEARCH ARTICLE

Statistical analysis of CPT tip resistances

Imre Laufer

Received 2012-05-10, accepted 2012-08-25

Abstract

Selecting proper values for soil parameters is a crucial aspect in geotechnical engineering. Geomaterials exhibit an inherent, natural variability, which can be assessed by statistical methods. CPT data lend themselves well for statistical analysis, given the large amount of data retrieved in a single test. The aim of this study was to examine the guidelines for statistical parameter estimation set out in Eurocode 7, as applied to CPT tip resistances. First, the guidelines and methods for estimation of fractiles and mean value with a given confidence level were reviewed. Second, a number of 125 CPT datasets were analyzed: the goodness-of-fit tests have shown that the common assumption of a normal distribution does not hold. Third, different estimation methods for the 5% fractile, the mean and the median were evaluated with regard to robustness and efficiency.

Keywords

CPT testing · tip resistance · characteristic value · statistical tests · nonparametric methods · parameter estimation

Imre Laufer

Budapest University of Technology and Economics, Department of Geotechnics, H-1111 Budapest, Műegyetem rkp. 1., Hungary
e-mail: imre.laufer@lambda2.hu

1 Introduction

The usual degree of uncertainty in a geotechnical model, involving stratification, soil properties and derived soil mechanical parameters, etc. is considered larger in contrast to uncertainties around geometrical and material properties in structural engineering. Site investigation methods – be they either field measurements or laboratory tests on samples - aim to reduce this uncertainty to a level which is considered acceptable for a specific task, but the highly variable nature of geomaterials and the low volume of ground tested – in contrast to the volume affected - still leave us with a substantial degree of ambiguity. Consequently, the role of engineering judgement in a geotechnical model is more pronounced.

However, engineering judgement, opinion, not to speak of beliefs not supported by analysis of available data might alone be very misleading, as the results of a survey reported by Fellin show [1]. In that survey, a table containing the results of classification and ring shear tests on a glacial till from Nothern Germany were sent to the participants. They were then asked to provide shear parameters (friction angle and cohesion) they would use in a slope stability analysis, based on the data from the table. The range of the answers for the friction angle contained even larger values than the maximum in the dataset.

An overview on the factors that influences people's and experts' judgement is presented in [2]. The short summary about expert opinions is the following: with sufficient training and feedback, one can develop a "well calibrated" estimation skill, but this usually does not apply to other fields and new tasks. Conducting a statistical analysis of the available data – both "new" data and "a priori" information – can substantially contribute to dealing with and quantifying some uncertainties in a geotechnical model. This applies all the more to CPT soundings, where one important task is estimating recurrence probabilities from the data plots.

1.1 General guidelines for parameter estimations

Design codes currently regarded as up-to-date try to address the aforementioned uncertainties with guidelines for selecting representative values for design; primarily for material strength

and stiffness, but also for geometrical properties. In this section, the corresponding rules of Eurocode 7 will be outlined, to set up the framework for the analysis of the CPT soundings.

The general principles for the selection of characteristic values for material properties – both engineered materials and geomaterials – are defined in the standards Eurocode 0 and Eurocode 7 themselves, and are explained in depth in numerous designers' guides, e.g. [3, 4], or [5], and papers, e.g. [6] and [7]. The characteristic value for a main property – which controls the occurrence of a particular limit state – should be selected such that the probability for a more unfavourable value must not exceed 5%. In statistical terms, this means finding the 5% fractile of a distribution when a low volume of ground is involved in the limit state, i.e. the loads cannot be redistributed. If the structure allows for load redistribution, or a large volume of ground is affected, then the value of the soil property should be selected "with confidence level of 95%".

The term "large" or "small" with respect to affected ground volume is not defined precisely, but rather left to engineering judgement. Fellin [1] presents a very illustrative and simple model on this matter: if a group of equally weighted boxes having different friction coefficients is pushed, then slip occurs if the pushing force exceeds the frictional resistance calculated from the average of the friction coefficients (spatial mean). This refers to the case with "large" volume involved. If however the boxes cannot transmit tension among each other, and they are being pulled, then the friction coefficient of the first box controls the slip resistance. If the boxes can be in a random order, then the smallest friction coefficient can be used for a lower bound estimate of the pulling force. This again refers to the case with "small" volume involved, or local failure. If we wish to link the affected volume with statistical concepts, then the rate of natural fluctuation (aleatory uncertainty) or periodic trend of the governing parameters could be used for comparison. Comprehensive explanations on this are also given in [3, 4], or [6].

Generally a lower value of a parameter (mainly strength parameters) will be more unfavourable, so the focus will be on deriving the (lower) 5% fractile and the lower bound of the 95% confidence interval for the mean. The statistical methods for the two above cases are different: the first involves making a point estimate for a fractile, the latter consists of setting up a confidence interval for a distribution parameter. (In the case where higher values would be more unfavourable, the methods are the same, except that the 95% fractile and the upper bound for the confidence interval are sought).

1.2 CPT and CPTu soundings

In geotechnical site investigation, the CPT (Cone Penetrometer Test), and more increasingly the CPTu (CPT with pore pressure measurement) sounding is becoming a standard tool.

The main concept of the method is pushing a steel rod with a conical tip into the ground, and recording the cone tip resistance q_c, the sleeve friction f_s and in CPTu soundings the pore pressure u around the cone. The reference configuration which is in widespread use today has an apex angle of 60°, a tip projection area of 10 cm^2, a friction sleeve area of 150 cm^2, and the value of the pore pressure, u_2 is measured at the cone shoulder. The pushing speed is 20 mm/s +5 mm/s for CPT, but for CPTu soundings a smaller tolerance is desired. The recording frequency of the data is usually 20 mm, but also very often 10 mm. A detailed description of the specifications can be found for example in [8].

The versatility of the testing method is reflected in the multitude of applications of the results. Earlier it was regarded as an aid alongside drilling in site investigation, but by now it has gained the rank of a standalone method.

One main field of application is geostratigraphic profiling, soil classification, and exploration of hydrogeological conditions. For this end, numerous profiling charts have been established and are in use. They are based on the cone tip resistance, the sleeve friction, their ratio R_f called friction ratio, or normalized cone resistance and friction ratio. Further details can be found for example in [9].

Other important fields of use in geotechnical engineering are the correlations between the cone tip resistance and other soil mechanical properties. These correlations are mainly based on regression analysis of CPT and laboratory or in-situ tests, and include an uncertainty which is expressed by the coefficient of determination R^2 of the regression. If used with proper caution (verifying the similar geological conditions and soil types of the site in question and of the ones used for setting up the correlations), as in-situ measurements, they can support and improve the selection of representative values in a geotechnical model. Furthermore, there are circumstances when no laboratory test results are available. In such cases, the geotechnical engineer has to rely on these correlations. Correlations have been developed between the CPT readings and a number of soil mechanical parameters: unit weight, friction angle, cohesion, undrained shear strength, stiffness properties, shear wave velocity, permeability, lateral stress coefficient, liquefaction potential, etc. An overview of these correlations can be found in [8, 9] and [10].

There are also direct applications for the CPT: design of deep and shallow foundations, evaluation of ground improvement measures, etc. [9–12].

It shall be emphasised that – in accordance with the guidelines in Section 1.1 – the variability of the soil parameters, namely cone tip resistance, has to be considered when selecting characteristic values during their application. As the correlations between CPT readings and other soil mechanical properties generally represent a connection between the expected values on the two sides, the measure of variability gets lost during such transformations. (And in turn, another uncertainty is introduced through the imperfect fit of the transformation, expressed by R^2.) Hence it is important to select the appropriate characteristic value before the transformation, from the CPT dataset.

In the next sections, the statistical background for selecting

the characteristic values will be investigated: the current statistical techniques and proposals in Eurocode 7 and the textbooks will be reviewed, along with some available evidence regarding CPT profiles. Then the results of statistical tests on CPT data will be presented. Finally certain options for selecting characteristic values – especially the mean estimated with a confidence level of 95% – in a setting with different assumptions than those made in the Eurocodes will be discussed.

2 Review of statistical techniques according to the Eurocodes

As mentioned in Section 1.1, a number of designers' guides and textbooks deal with the application of the principles and rules given in the Eurocodes. Regarding the statistical derivation of the characteristic values adopted for design, the standards themselves (EC 0 and EC 7) do not mention any kind of distribution to be used or preferred. The textbooks, however, state generally, or assume that the material properties in question are either normally or lognormally distributed. In the latter case, the statistical techniques can be applied to the transformed variables Y=lnX, where X are the original observations in the sample.

2.1 The 5% fractile

If the normality assumption holds, the 5% fractile – defined as $P(x \leq x_k) = 0.05$, meaning that the probability of a randomly selected x being smaller than the characteristic value x_k is 5% – can be calculated as follows:

$$x_k = \bar{x} - t_{n-1}^{5\%} \sqrt{1 + \frac{1}{n}} s_x \tag{1}$$

where $\bar{x}$ is the sample mean, s_x is the sample standard deviation, n is the sample size, and $t_{n-1}^{5\%}$ is the 5% fractile of the Student's t distribution with $n - 1$ degrees of freedom. If the standard deviation σ_x is a priori known, then the formula simplifies to

$$x_k = \bar{x} - 1.645 \sqrt{1 + \frac{1}{n}} \sigma_x \tag{2}$$

where 1.645 is the 5% fractile of the standardized normal distribution $N(0,1)$ having a mean of 0 and a variance of 1. With an increasing sample size n, (1) converges to (2) from above. The difference rises fast for small samples (approx. $n<10$) [3]. This method is called the prediction method. A formally similar classical technique is the so-called coverage method, which takes into account the uncertainty of the parameter estimation.

A more general method for estimating the 5% fractile is the so-called method of order. It does not make any assumptions for the type of distribution; it only requires "sufficient" data. The sample is ordered: $x_1' \leq x_2' \leq x_3' .. \leq x_n'$, and the value of the empirical cumulative distribution function (CDF) is assigned to the i-th element as $i/(n + 1)$. Then the 5% fractile will be the greatest element with $i/(n + 1) \leq 0.05$. In this sense, "sufficient" means that there should be enough values to properly encompass the probability 0.05: $n \geq 20$. For further reference, see [5].

2.2 The mean value with a confidence level of 95%

The estimation of the mean with a certain confidence level requires the construction of a confidence interval for the distribution parameter (which is the mean in this case). The confidence level 1-ε – in this case 95% – indicates an error probability of $\varepsilon \quad - \varepsilon = 5\%$. In this case ε is the probability of the true mean lying outside the confidence interval. In statistics, the dual problem to the construction of confidence intervals is hypothesis testing: an associated hypothesis test can be constructed to each confidence interval and vice versa (although not always practicable). Consecutively, the associated hypothesis test also has a significance level of 1-ε. Here, ε is the probability of the Type I error, falsely accepting the hypothesis H_0.

The confidence interval defined as

$$P\left(\mu_{low} \leq \bar{x} \leq \mu_{high}\right) = 95\% \tag{3}$$

has an associated hypothesis test

$$H_0 : \mu = \bar{x} \text{ versus } H_1 : \mu \neq \bar{x} \tag{4}$$

with a significance level of 95% [13]. In the expression (3), μ_{low} and μ_{high} define an interval for the mean values which may have generated the sample, and cannot be discredited with a probability of 95%. Discredited means rejected by the hypothesis test (4), where the null-hypothesis (H_0: the true mean not being significantly different from $\bar{x}$) has an error probability of 5%, and an acceptance region of $\left[\mu_{low}, \mu_{high}\right]$. This hypothesis test is called a two-tailed test, because the rejection region has one $\varepsilon/2$ part in the lower and one $\varepsilon/2$ part in the upper tail of the distribution, see Fig. 1.

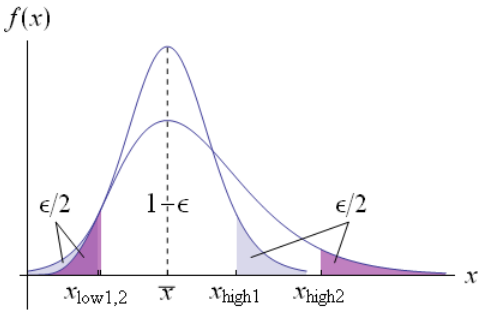

Fig. 1. Two-tailed confidence intervals (in case of a symmetrical and an asymmetrical distribution) for x

In certain cases one is not interested in the higher bound μ_{high}, thus the appropriate hypothesis test will be one-tailed:

$$H_0 : \mu = \bar{x} \text{ versus } H_1 : \mu < \bar{x} \tag{5}$$

and the 95% confidence interval "simplifies" to a 5% fractile:

$$P\left(\mu_{low} \leq \bar{x}\right) = 5\% \tag{6}$$

Which one should be used for selecting the characteristic value is not stated exactly in Eurocode 7. In many cases – e.g. strength properties – (5) will be appropriate. Conversely, if both low and high values are of importance – e.g. for stiffness properties –,

then the right choice is (3). This can also be seen from equation (8): if the sample is normally distributed and thus symmetric, then the t-test – based on the Student t distribution – can be applied for the hypothesis test. Here, the value 1.645 is the critical value for both the one-tailed test with 95% significance level and the two-tailed test with 90% significance for $n = \infty$. This argument is also made in [1] with the conclusion of selecting a two-tailed 90% confidence interval. The statement "with a confidence level of 95%" lacks the definition of the interval being either one- or two-tailed. From the above, the two-tailed, 90% (central) confidence interval is evident.

Again, if the normality assumption holds, the mean value can be estimated at a confidence level of 95% in the case of unknown standard deviation with

$$x_k = \bar{x} \pm t_{n-1}^{5\%} \sqrt{\frac{1}{n}} s_x \tag{7}$$

or in the case of known standard deviation with

$$x_k = \bar{x} \pm 1.645 \sqrt{\frac{1}{n}} \sigma_x. \tag{8}$$

These formulae are quoted for example in [3, 4] or [6] and [7]. These sources also mention a similar technique for making estimations of the mean if a linear trend is present in the data, and [3] contains techniques for dealing with small datasets (there, a dataset is regarded "small" if n<13).

If the data is normally distributed, then the technique for setting up the confidence interval is well established. However, if the distribution departs from normal, using the formulae (5) and (8) requires some additional considerations. This issue will be discussed further in Section 4.

2.3 Statistical considerations and tests

An important point made in EC 7 is the need for incorporation of previous knowledge, experience and engineering judgement in the process of selecting characteristic values. One possibility may be using Bayesian methods, described e.g. in [3, 6] and [14], but that may be too complicated for use in everyday tasks. Simple options include comparing the standard deviation with literature data, selecting the "standard deviation known" case for the calculations with variation coefficients ($\nu_x = \sigma_x / \bar{x}$) from literature, or using Schneider's approximation described in the designers' guides mentioned above. Coefficients of variance for a number of parameters derived from large repetition test series are given e.g. in [3, 6], and detailed compilations are presented in [2] and [14].

The assumption of a normal distribution is emphasised in the designers' guides above, but unfortunately, neither its verification nor the consequences of the deviation from it are addressed. The underlying reason behind that may be that usually the practicing geotechnical engineers have neither access to sufficient measurements, nor in-depth statistical knowledge to carry out normality or other goodness-of-fit tests. [5] contains a reference to other standards for normality tests, but they are not presented in the book itself. The book also deals with the use of the log-normal distribution (both with the 2-parameter-case, with lower bound at 0, and the general 3-parameter-case), and shows how the skewness of the distribution affects the 5% fractile. Generally, if the skewness is positive, the 5% fractiles estimated with a normal distribution will be smaller than the actual values (favourable error), and for a negative skewness the error will be unfavourable (overpredicted value). It is also suggested that the normal distribution may be applicable if the skewness is smaller than ±0.1.

A good example of rigorous testing of the normality assumption in a quantitative way is given in [15]: after a visual examination (for example on a probability grid, or examining the histogram – also called wittily "chi-by-eye"), the Anderson-Darling A^2-test is employed to set the confidence level of 95%. Furthermore, the Shapiro-Wilk test can be applied for small datasets; or other general – and less powerful – goodness-of-fit tests, such as the χ^2-test, or the Kolmogorov test, as described e.g. in [14].

For routine use, the tests for the 3rd and 4th central moments of the sample (the skewness and kurtosis), described in [16] can be useful.

The results of goodness-of-fit tests and their Pearson-plot (explained in Section 3.2) for a number of soil mechanical properties are given in [14]: the tanφ and cohesion were found to be beta-distributed, and other parameters followed beta-, gamma-, lognormal, normal and uniform distributions. [2] also presents similar evaluations with similar results. Here, the distributions derived for φ are normal, beta-, uniform and gamma-distributions. Distributions for raw and detrended data from SPT and CPT tests are also presented, with a similarly wide range of results.

3 Analysis of CPT data

As seen above, statistical techniques described in Section 2.1-2.2 are based on assuming a normal distribution for the property in question. This may apply more or less well for many soil properties, but is not well supported for CPT data. For this end, goodness-of-fit and classification tests were carried out on cone tip resistances from a total of 125 homogeneous soil layers.

CPT data lend themselves well to statistical analysis: in statistical textbooks, a sample is regarded "large" above 20-30 observations. With the usual sampling interval of 2cm in CPT testing, this applies for layers with thicknesses above 40-60cm.

3.1 CPT data, filtering

The CPT soundings analyzed in this study were carried out for 2 projects in Hungary: 6 CPTs and 6 CPTu-s were sunk at an industrial site, and 34 CPTu soundings were carried out for a road construction project along an approx. 32km–long route. The soundings on the industrial site reached depths between 19.5-25.8m, on the loess-plateau along the Danube with a deep-lying

water table. The penetration tests for the road project were sunk to depths between 17.5-30.1m, with variable geological and hydrogeological conditions.

The layers were selected for analysis if the soil types from the CPT and nearby boreholes matched, giving 44 datasets for the industrial site and 81 for the road route, a total of 125 datasets. The reading intervals in each case were 20mm. The soil type classification in the CPTs was performed according to the Robertson 1986 chart [9], with corrected cone resistances:

$$q_t = q_c + u_2(1 - a) \tag{9}$$

where q_c is the measured cone tip resistance, and a is the cone area ratio, see [8]. For the industrial site, the q_c-values were used, because either u_2 was not recorded, or a was not available. This correction is of importance predominantly in soft soils under the water table, but this was not the case here.

It is understood that increasing the overburden stress increases the tip resistances, which may bias the results of CPT-based soil classification. That is especially true for very thick or deep-lying layers, and several normalization techniques have been proposed to account for this effect. They are presented e.g. in [10]. Usually, normalization requires the knowledge of the bulk density of the soil, the groundwater level and groundwater regime to calculate total and effective overburden stresses. Due to uncertainties in the latter, and due to the fact that most profiling charts were developed for shallow and moderate depths (<30m), [9] suggests that normalization does not necessarily improve the accuracy of profiling. In a "homogeneous" soil layer, the effective overburden stress increases linearly with depth, at a rate of γ ≈14-21 kN/m^3 above the groundwater table. None of the datasets came from large depths and even for the thickest layer with a thickness of 13.60m the change in effective overburden stress should not exceed ≈290 kPa. In contrast, the mean tip resistance for the vast majority of the datasets ranges between q_t ≈1 500–11 000 kPa, and the change in overburden stress inside a layer falls in the range of aleatory fluctuations. However, this effect could not be neglected in very soft layers.

The soil profile at the industrial site comprises loessy, low plasticity clay with consistencies ranging from hard to soft (denoted A: hard – B: firm – C: soft – D: firm – E: hard with increasing depth).

The soil layers from the road route form a "continuum" between medium plasticity clays and fine to medium sands. The layers in each profile are denominated with increasing depth consecutively as A, B, C... etc, without any further meaning of the notation.

The soil layers with depth and soil type are given in the Appendix, Tables 4 and 5.

The proper statistical treatment of the data requires the screening out of outliers. A general discussion, as well as statistical techniques for this are presented e.g. in [14]. If a physical justification can be given for a suspect outlier, it may be removed or corrected. In a CPT test, outliers are produced during the attachment of extension rods to the cone shaft: a steep drop in the cone resistances is produced at regular intervals (approx. 90cm), producing a "sawtooth" pattern, see Fig. 2. This error is usually automatically corrected with newer data logging equipment; for the present analysis, these readings were dropped. However, this correction can occasionally lead to gaps in the range of the measured values (see below, in Section 3.2.3).

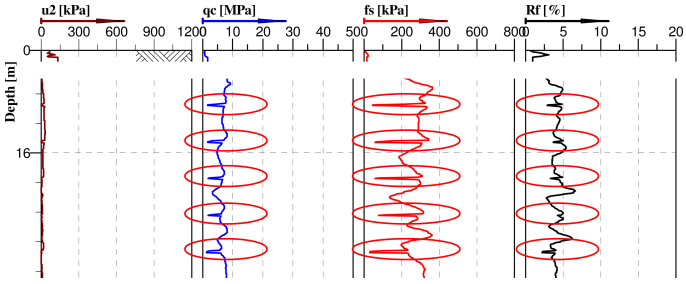

Fig. 2. Sawtooth pattern in a CPT diagram, due to attachment of extension rods

On the other hand, even very "strange" readings may be traced back physical roots: for example cobbles or gravel in a clayey deposit may produce outstandingly high tip resistance, or cavitation of the pore water. [8] Sharp fluctuations in cone resistance are also typical for sand soils. In addition, the type of distribution also influences the statistical decision about outliers – distributions with heavier tails are more "tolerant" against outliers. Therefore, to avoid the influence of the goodness-of-fit tests with more or less subjective rejection of suspect values, no further screening out of outliers was done.

Also, the values at layer boundaries were left unaffected, even though there are both experimental and theoretical evidence for interfaces modifying the "true" cone tip resistance [8].

3.2 Goodness-of-fit tests

In order to verify or reject the normality assumption, and more broadly, in search for a well-fitting distribution, the datasets were analyzed in the Pearson coordinate system, and Kolmogorov tests were carried out for 13 continuous distribution types. The tested distributions are listed in Table 1, with their most important details. The notations and names in Table 1 follow the expressions used in the program Mathematica 7.0 [17].

A literature research regarding possible distributions also encourages a departure from the normality assumption: Mortensen et al. (reported in [8]) found – after smoothing and thorough filtering – that the lognormal distribution suits their data on clay tills very well. [2] reports the results for CPT tests in mine tailings, on both raw and detrended data. The distributions passing the Kolmogorov test "at 5% level" are the beta- and lognormal distributions for the raw data, and normal, lognormal and beta-distributions for the residuals after trend removal. In certain cases, no distribution passed the test at the given significance level. The lognormal distribution might also be inferred from the

Tab. 1. Overview of the distributions tested in the analysis ($B()$ is the beta-function, $\Gamma()$ is the gamma-function, and $\zeta()$ is the Riemann zeta-function)

Name	*Parameters*	*PDF*	*Support*	*Estimation*	*Pearson* β_1	*Pearson* β_2
Beta	a, b, α, β	$\frac{1}{B(\alpha,\beta)} \frac{(x-a)^{\alpha-1}(b-x)^{\beta-1}}{(b-a)^{\alpha+\beta-1}}$	$[a, b]$	ML-Eq numerical	region	
Cauchy	a, b	$\frac{1}{b\pi\left(1+\frac{(x-a)^2}{b^2}\right)}$	$(-\infty, \infty)$	ML-Eq numerical	–	–
Extreme Value	α, β	$\frac{1}{\beta} e^{-\frac{x-\alpha}{\beta}} e^{-e^{-\frac{x-\alpha}{\beta}}}$	$(-\infty, \infty)$	ML-Eq numerical	$\frac{864\zeta(3)^2}{\pi^6}$	5.4
Gamma	α, β	$\frac{1}{\Gamma(\alpha)} x^{\alpha-1} \beta^{-\alpha} e^{-\frac{x}{\beta}}$	$[0, \infty)$	ML-Eq numerical	$\frac{4}{\alpha}$	$3 + \frac{6}{\alpha}$
Gumbel	α, β	$\frac{1}{\beta} e^{\frac{x-\alpha}{\beta}} e^{-e^{\frac{x-\alpha}{\beta}}}$	$(-\infty, \infty)$	ML-Eq numerical	$\frac{864\zeta(3)^2}{\pi^6}$	5.4
Inverse Gauss	μ, λ	$\frac{1}{\sqrt{2\pi}} \sqrt{\frac{\lambda}{x^3}} e^{-\frac{\lambda(x-\mu)^2}{2x\mu^2}}$	$(0, \infty)$	ML-Eq analytical	$\frac{9\mu}{\lambda}$	$3 + \frac{15\mu}{\lambda}$
Laplace	μ, β	$\frac{1}{2\beta} e^{-\frac{(x-\mu)\mathrm{Sign}[x-\mu]}{\beta}}$	$(-\infty, \infty)$	ML-Eq analytical	0	6
Logistic	μ, β	$\frac{e^{-\frac{x-\mu}{\beta}}}{\beta\left(1+e^{-\frac{x-\mu}{\beta}}\right)^2}$	$(-\infty, \infty)$	num.max. $l\left(\hat{\theta}\right)$	0	4.2
Lognormal	μ, σ	$\frac{1}{\sqrt{2\pi}x\sigma} e^{-\frac{(\ln x-\mu)^2}{2\sigma^2}}$	$(0, \infty)$	$Y = \ln(X), \rightarrow$ Normal	$(e^{\sigma^2}-1)\cdot(e^{\sigma^2}+2)^2$	$e^{4\sigma^2} + 2e^{3\sigma^2} + 3e^{2\sigma^2} - 3$
Maxwell	σ	$\sqrt{\frac{2}{\pi}} \frac{x^2 e^{-\frac{x^2}{2\sigma^2}}}{\sigma^3}$	$[0, \infty)$	ML-Eq analytical	$\frac{8(16-5\pi)^2}{(3\pi-8)^3}$	$\frac{-192+\pi(16+15\pi)}{(8-3\pi)^2}$
Normal	μ, σ	$\frac{1}{\sqrt{2\pi}\sigma} e^{-\frac{(x-\mu)^2}{2\sigma^2}}$	$(-\infty, \infty)$	ML-Eq analytical	0	3
Rayleigh	σ	$\frac{1}{\sigma^2} x e^{-\frac{x^2}{2\sigma^2}}$	$[0, \infty)$	ML-Eq analytical	$\frac{(\pi-3)^2\pi}{2(2-\pi/2)^3}$	$\frac{32-3\pi^2}{(4-\pi)^2}$
Weibull	α, β	$\frac{\alpha}{\beta}\left(\frac{x}{\beta}\right)^{\alpha-1} e^{-\left(\frac{x}{\beta}\right)^{\alpha}}$	$[0, \infty)$	ML-Eq numerical	see text	

various soil classification charts for CPT: most of them use log-scale for the tip resistance (e.g. Robertson, Eslami&Fellenius charts); or layer boundary search methods [18].

Eventual trends with depth were not removed from the data in the current research, for the following reasons. Sometimes – e.g. for the calculation of the pile shaft resistance – only the average value is relevant. If a (linear) trend is present, then the estimation of the trend itself is of importance, and the distribution of the residuals is of less concern. A linear trend may be estimated e.g. with the methods given in [4], and the assumption of normally distributed residuals in regression analysis is a robust one (small deviations little affect the results). If the residuals are far from normal, a transformation of the variables may be helpful [19]. Furthermore, as noted in [20], the selection of a trend is not unique, but not completely arbitrary either: it's left to the reasonable judgement of the analyst.

3.2.1 Pearson plot

A preliminary choice for the distribution type can be obtained from the Pearson coordinate system. The idea behind it is that most distributions are well described by their first 4 moments or central moments: mean value μ, variance σ_x^2, skewness γ and kurtosis κ. Their bias corrected estimates are:

$$\begin{aligned} \bar{x} &= \frac{1}{n}\sum_{i=1}^{n} x_i, \quad s_x^2 = \frac{1}{n-1}\sum_{i=1}^{n}(x_i-\bar{x})^2, \\ \gamma &= \frac{n\sum_{i=1}^{n}(x_i-\bar{x})^3}{(n-1)(n-2)(s_x^2)^{3/2}}, \\ \kappa &= \frac{n\sum_{i=1}^{n}(x_i-\bar{x})^4}{(n-1)(n-2)(s_x^2)^2} \end{aligned} \tag{10}$$

Here, the normal distribution has κ =3. The coordinates in the Pearson system are $\beta_1 = \gamma^2$ and $\beta_2 = \kappa$. The coordinate system is divided into 7 regions, which indicate the so-called Pearson-family of distributions suitable for reproducing the first 4 moments of a sample [2]. Also, the trace of any distribution can be plotted by calculating their respective β_1 and β_2 coordinates: they evaluate either as points, curves or regions depending on the parameters of the distribution (see Fig. 3).

The 13 distribution types have been chosen to cover a wide range of possible distributions; linking the physical background of the investigated distributions to the CPT measurements was not a primary concern. Some of them have few and easy-to-fit parameters, others offer more adaptability. Adaptability can be tied more or less to the trace in the Pearson coordinate system: distributions appearing as points offer the least adaptability, while the ones covering a region are more flexible to reproduce observations, and those describing a curve lie in between. From the 13 distributions tested, the normal, logistic, Laplace-, Rayleigh-, Maxwell-, Gumbel-, and extreme value distributions evaluate as points; the lognormal, gamma, Weibull-, and inverse Gaussian distributions evaluate as curves; and the beta distribution covers the whole region I in the coordinate system. It must be noted, however, that the trace of the Weibull distribution behaves almost as a point with usual values for α.

On the other hand, the flexibility of the distributions strongly depends on the number of their parameters: more flexibility is achieved mainly through more parameters, which need to be fitted. The fitting procedure will be explained later, at the discussion of the Kolmogorov tests. The Pearson plots of the datasets (Fig. 4) show a tendency for the points to be concentrated close to $\beta_1 = 0$ (symmetrical distributions), and mainly in the band of the beta distributions. This is also consistent with the results presented in [2]. Plotting the skewness γ and the kurtosis κ against the length n of each dataset (Fig. 5), no strong correlation can

be found. The $\gamma - \kappa$-plot shows that there is a tendency towards positive skewness.

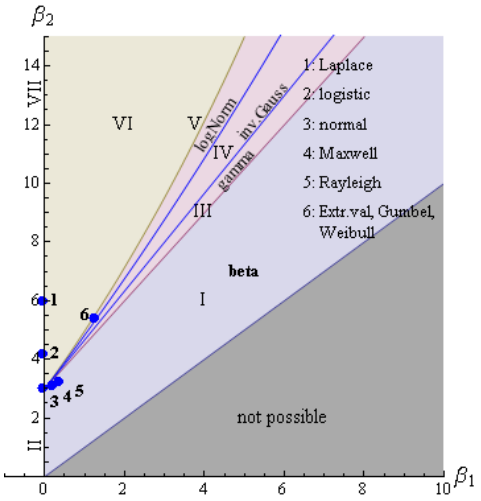

Fig. 3. Traces of distributions in the Pearson coordinate system

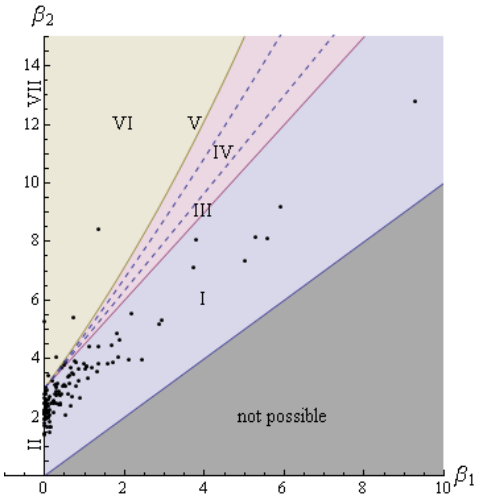

Fig. 4. Datasets in the Pearson coordinate system

Based on the examination of the Pearson plot, most of the listed distributions appear suitable, with traces of the Laplace-, the Weibull-, extreme value-, Gumbel-, and the logistic distributions lying apart from the bulk of the points.

3.2.2 Kolmogorov tests

The goodness-of-fit is better expressed in quantitative terms, and for this end, Kolmogorov tests were applied to each dataset. This test was chosen over the other common test, the χ^2-test for a number of reasons. First, because it requires less logical decisionmaking: in the χ^2-test, each bin should contain more than 3 (or 5) observations, this in turn affects the subdivision of the support of the chosen distribution into bins. Second, the χ^2-test lumps together the information from the observations in a bin, while the Kolmogorov test considers each observation separately. (Following this train of thought, the Pearson plot lumps all observations into the β_1 and β_2 coordinates.) Third, it is reported to be less rigorous than the χ^2-test, which is – in the light of the results – not a drawback. (Further reference on this shall be made e.g. to [13] and [14].)

The Kolmogorov test is based on the greatest difference D_n between the empirical CDF and the hypothesised CDF F_θ:

$$D_n = \max_i \left[\max \left(\left| \frac{i-1}{n} - F_\theta\left(x_i'\right) \right|, \left| \frac{i}{n} - F_\theta\left(x_i'\right) \right| \right) \right] \tag{11}$$

where x_i' is the i-th element in the sequence of the ordered observations ($x_1' \leq \cdots \leq x_n'$). The expression

$$z = D_n \sqrt{n} \tag{12}$$

follows a distribution described by the Kolmogorov function

$$K(z) = \begin{cases} 0 & \text{if } z \leq 0 \\ 1 - 2\sum_{j=1}^{\infty} (-1)^{j-1} e^{-2j^2 z^2} & \text{if } z > 0 \end{cases} \tag{13}$$

The value

$$p = 1 - K(z) \tag{14}$$

yields the confidence level for the observations stemming from the distribution $F_\theta(x)$. (In other words, it is the significance level of the hypothesis test $H_0 : P(X < x) = F_\theta(x)$ vs. $H_1 : P(X < x) \neq F_\theta(x)$) [13].

At first sight, the concise notation $F_\theta(x)$ in (7) hides the fact that the Kolmogorov test is a so-called parametric test, i.e. the distribution type F_θ is assumed to be known, and values for the parameters θ have to be selected prior to the test. This calls for a "plug-in" parameter estimation procedure. The parameter estimation procedure adopted in this research is the maximum likelihood-method, and the estimations $\hat{\theta}$ for the parameters are called maximum likelihood-estimators (MLEs).

At the core of the maximum likelihood-method lies the likelihood function

$$l_\theta(x_i) = \ln \prod_{i=1}^{n} f_\theta(x_i) \tag{15}$$

where $f_\theta(x)$ is the probability distribution function (PDF) of the chosen distribution. The aim is to select the values $\hat{\theta}$ which maximize the joint likelihood of the observations to happen. The log-form is convenient because the application of logarithmic identities enables considerable simplifications on the right-hand-side of (15). From this point, the general procedure is to calculate the partial derivatives $\frac{\partial}{\partial\theta} l_\theta(x_i)$, and solving the likelihood-equations

$$\frac{\partial}{\partial\theta} l_\theta(x_i) = 0 \tag{16}$$

either analytically (if practicable), or – more often – numerically. Table 1 indicates which solution was used for each of the 13 distributions. For the lognormal distribution, the observations were first transformed with $Y = \ln X$, and then they were treated as normally distributed. In case of the logistic distribution, the expression (15) was maximized numerically due to poor convergence during the solution of (16).

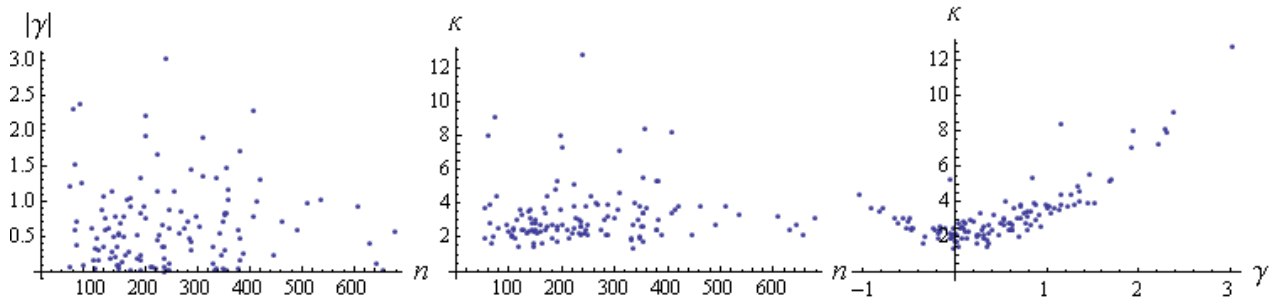

Fig. 5. Skewness and kurtosis plots against *n*, and against each other

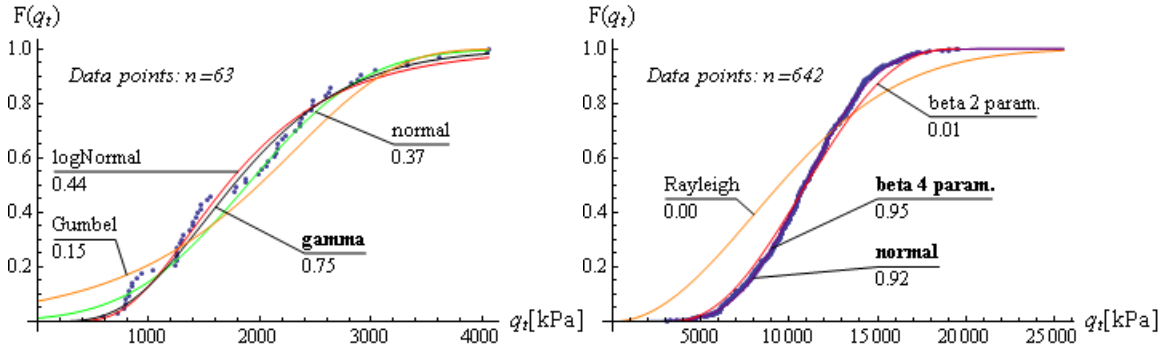

Fig. 6. Examples for a short and a long dataset, and fitted distributions (with goodness-of-fit indicated)

Despite the fact that computing the MLEs requires a considerable effort, they have a very favourable property: they are so-called minimum variance, asymptotically unbiased estimators [13]. Practically, this can be interpreted as the MLEs being the best estimators available.

3.2.3 Evaluation of the results

Each of the 125 datasets was cross-tested with each distribution type. The MLEs for each distribution have been calculated with (15) and (16) for each and every dataset, and the Kolmogorov-test (11)-(14) for each distribution has been performed using the corresponding MLEs. Although the number of distribution types was 13 (see Table 1), 14 tests were conducted for each dataset: for the beta distribution, one case included estimating all 4 parameters through MLE; while in the second case the lower and upper bounds a and b were fixed close to the observations, with $a = x_1' - 0.01$ and $b = x_n' + 0.01$.

Fig. 6 shows 2 examples of the datasets and fitted distributions: one for a short dataset, and another for a long one.

Comparing the results among each other is not quite straightforward: expression (12) shows that the value of the Kolmogorov function (13) increases with the length of the dataset n. In other words, longer datasets have to fit more smoothly to the theoretical distribution than short ones to reach the same significance level. Furthermore, the CPT equipment and testing procedure bear an intrinsic variability, or "noise", which leads to random reading errors with a variation coefficient of ~8-22%. [2]. Also, some datasets are "gap-graded" (contain jumps in their CDF), which diminish the achievable level of fit for any continuous distribution.

To cope with these difficulties, the performance of the tested distributions was evaluated with 3 scores, given in Table 2.

First, the score allocated to a distribution was the number of times it proved to be the best-fitting one. (Note: The column sums up to 127 instead of 125, because in 2 cases the 4-parameter and the 2-parameter beta distributions reached the same level of fit.)

Tab. 2. Overview of the Kolmogorov tests (* see note above)

Name	Times best	Averages	
		Max norm	Sum norm
Beta 4 parameter	42*	0.583	0.231
Beta 2 parameter	6*	0.167	0.059
Cauchy	5	0.112	0.049
Extreme Value	12	0.305	0.099
Gamma	8	0.286	0.069
Gumbel	10	0.143	0.043
Inverse Gaussian	6	0.266	0.069
Laplace	5	0.150	0.049
Logistic	13	0.370	0.105
Lognormal	7	0.310	0.083
Maxwell	3	0.072	0.017
Normal	3	0.237	0.058
Rayleigh	1	0.019	0.004
Weibull	6	0.250	0.065

However, a large amount of information about the performance of the distributions is lost in this approach. To consider all of the Kolmogorov test results, they were normalized with respect to their maximum value and their sum for each dataset. The weight or score for a distribution was then calculated as

$$w_j^{max} = \frac{p_j}{\max_j \left(p_j\right)} \tag{17}$$

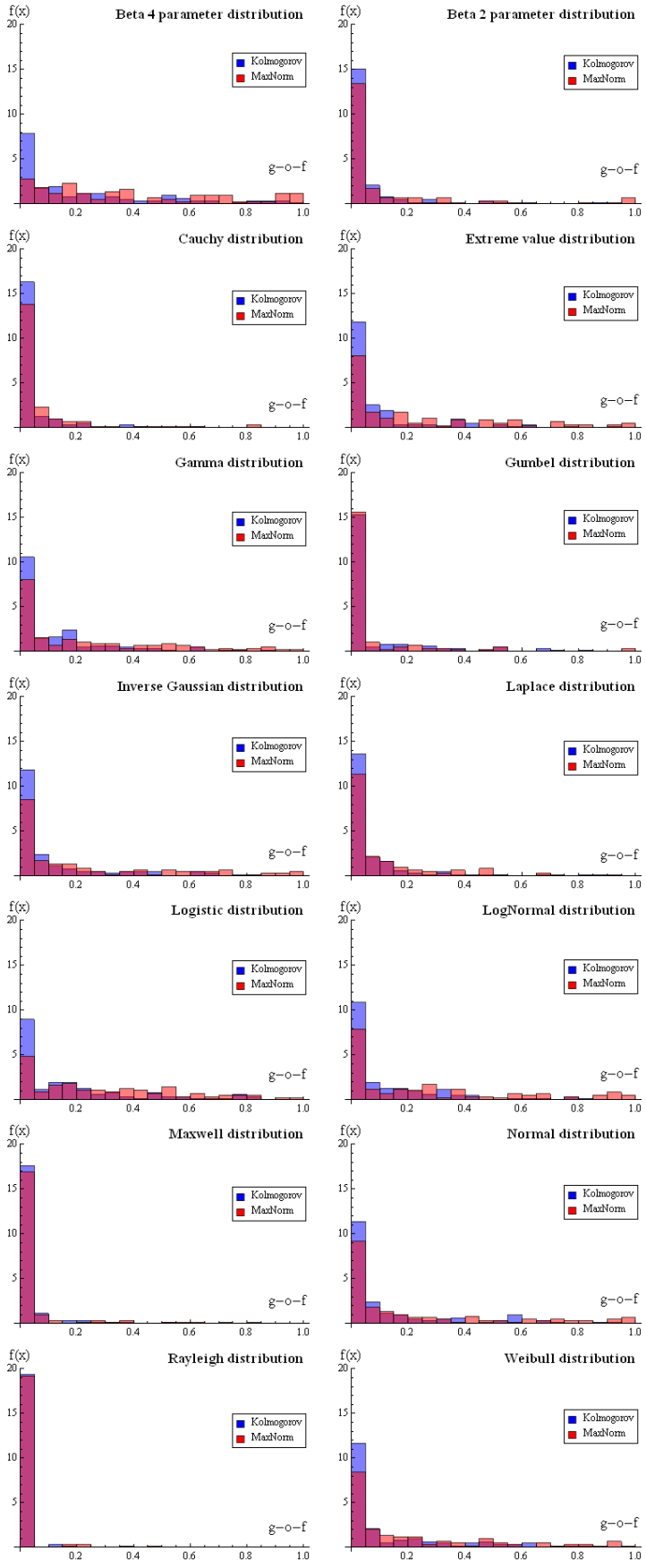

Fig. 7. Histograms of the goodness-of-fit (g-o-f) values and their max-norm weights

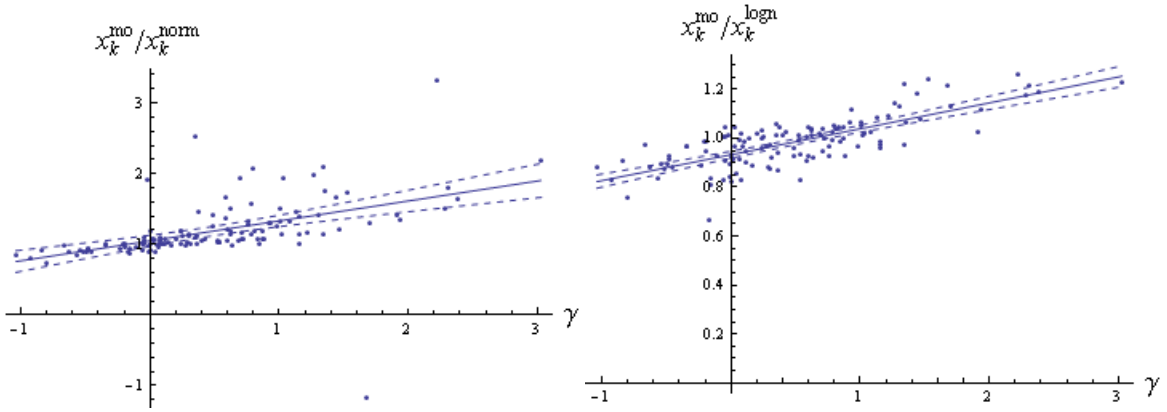

Fig. 8. Ratios of x_k^{mo} method-of-order 5% fractiles to x_k^{norm} normal and x_k^{logn} lognormal distribution 5% fractiles

$$w_j^{sum} = \frac{p_j}{\sum_{j=1}^{14} p_j} \tag{18}$$

Here, $p_j$stands for the result of the Kolmogorov test for the j-th of the 14 distributions tested ($j = 1 \ldots 14$). These normalizations allow for "evening out" the differences between the datasets arising from different lengths, gaps, or noise. The weights calculated with the max norm (17) help to rank the performance of the distributions over all datasets: in each case, the best fit receives the weight 1, and the others get their weights according to the ratio of their respective fit probability. The sum norm (18) is more suitable for the comparison of the distributions for a given dataset: the closer its value is to unity, the more dominant it is among those tested. (In other words: a value close to 1 means that the distribution in question excels, whereas the others do not; it is a rough measure of certainty to choose the right one.) Of course, the two normalizations are not independent. It must also be stressed that they are only simple aids for the comparison. Their average values over all datasets are also listed in Table 2; higher averages indicate a better fit.

Plotting the histograms (Fig. 7) of the Kolmogorov test results (blue) and the max-normalized results (red) for each distribution gives the most insight into their performance. The first notable feature is that very low fit probabilities characterize each distribution, which can be explained by the reasons given above. If the histogram for the max-normed weights for a distribution is shifted to the right (upwards), it indicates a good fit, and if the two histograms overlap (no or very little shift can be observed), the overall performance of the distribution is not satisfying.

Table 2 and the histograms in Fig. 7 show that the beta distribution with 4 parameters stands out regarding its goodness-of-fit. It is followed by the logistic distribution, the extreme value-distribution and the lognormal distribution, ranked 2nd through 4th according to the max- and sum-norms.

Interestingly, the normal distribution performs rather poorly, taking the 8-9th ranks with the two norms. The inverse Gaussian, gamma, and Weibull distributions achieve intermediate scores, while the Cauchy, Laplace, Gumbel, and the 2-parameter beta distributions lie at the lower end of the list. The simple, one-parameter distributions, Rayleigh and Maxwell show a poor fit and thus are not suitable modelling CPT data.

Some considerations should be made regarding the best-performing distributions. The versatility of the 4-parameter beta distribution arises from the large number of parameters: the lower bound a and upper bound b have to be set by parameter estimation, in addition to α and β. This requires a considerable effort, since an analytical procedure does not exist for this end, they have to be approximated numerically. To investigate the sensitivity of the fit against their values, the 2-parameter beta distribution was also tested, where a and b were fixed close to the observed values. As seen in Fig. 6 and Table 2, this reduced the overall performance considerably. Furthermore, the values for a and b in the 4-parameter case occasionally took on improbable values, since they were only subject to constraints $0 < a < \min(x_i)$ and $\max(x_i) < b$.

The parameter estimation for the logistic distribution was carried out by maximizing the likelihood-function (15) itself, since the numerical solution of the likelihood-equations (16) often showed poor convergence. In turn, maximizing the likelihood-function resulted many times in computational under- and overflow problems, making a rescaling of the dataset necessary.

The extreme value distribution (and also the closely related Gumbel distribution) needs only the parameter β estimated numerically, α can then be calculated analytically, making the parameter fitting easier. The method-of-moments estimator for β is a good initial value for the numerical solution.

Estimating the parameters for the lognormal distribution is probably the easiest: first, the logarithm of the observations is taken, and the mean and standard deviation of the transformed values are calculated. Another advantage of the lognormal over the logistic and the extreme value distributions is that it can only yield positive values, which reflect the physical nature of CPT tip resistances.

Last but not least, the question arises: what values can be accepted as satisfactory in a goodness-of-fit test? Judged from the results of the Kolmogorov tests, and as shown in Fig. 6, values above cca. 0.35-0.40 can be tentatively accepted as satisfactory for CPT data. This holds for "shorter" datasets with

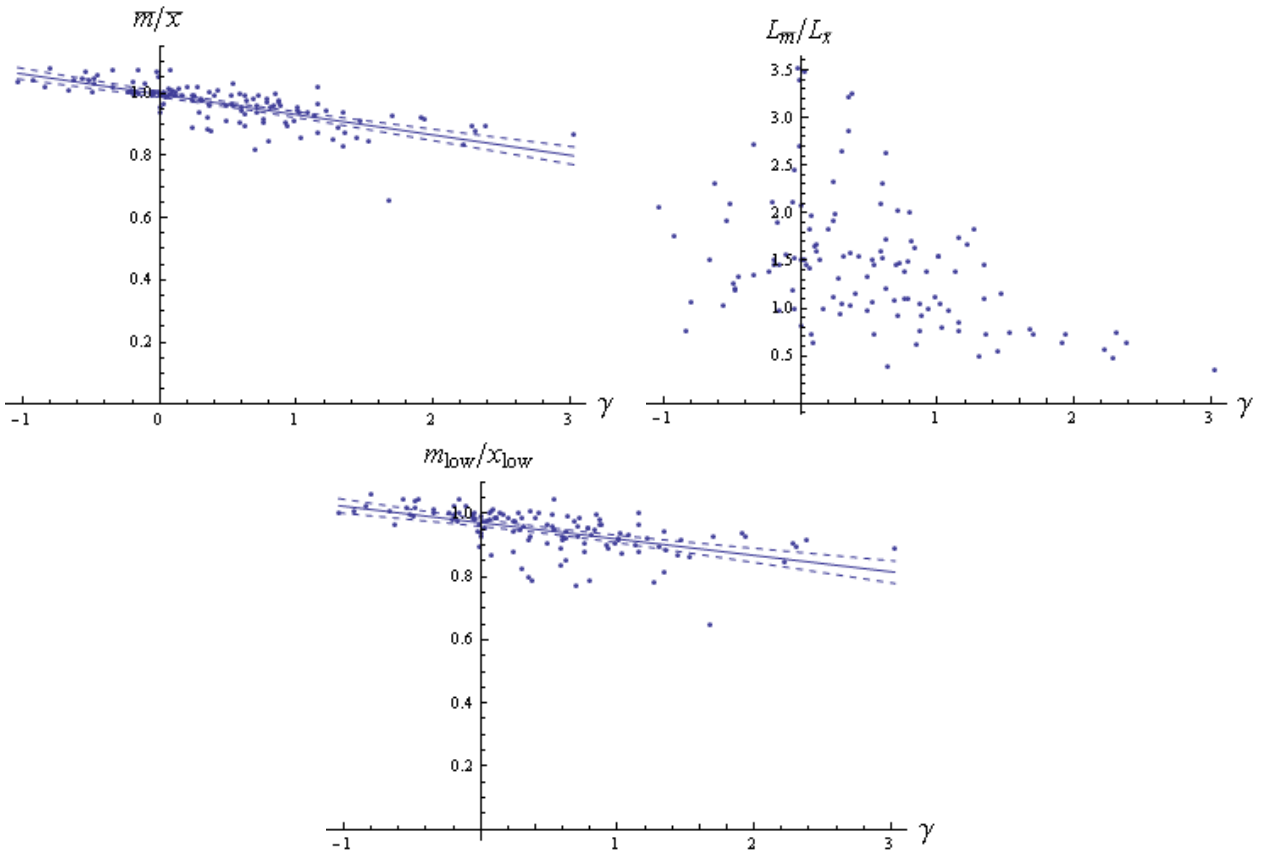

Fig. 9. Ratios of a) mean and median, b) length of confidence intervals and c) lower interval bounds

$n \approx 50 - 100$, but lower values can also be accepted for longer ones. In such cases, the decision of accepting or rejecting a distribution (with estimated parameters) can be confirmed by additionally inspecting the empirical and fitted CDF, as shown in Fig. 6.

As seen from the scattering results in Fig. 4, 5 and 7, none of the tested distribution types may be deemed superior to the others. The skewness and kurtosis of the datasets covers a wide range, and the best-fitting distribution type varies strongly. That leads to the question of how to conduct statistical inference in such an uncertain setting.

4 Estimation of characteristic values

4.1 Robustness and efficiency

If the underlying distribution for one or more datasets is unknown, one can make use of so-called nonparametric methods. The term nonparametric means that the type of distribution does not need to be known. In such a case, quantitative inference is still possible, but at the price of lower precision. Nonparametric estimators are often referred to as robust ones, expected to perform well for several types of distributions.

One possible measure of robustness is the (asymptotic) breakdown point: it gives the ratio of data points that can be changed arbitrarily while the estimator remains bounded. (It gives the ratio of eventually completely erroneous data that the estimator tolerates.)

The sample mean $\bar{x}$ has a breakdown point of 0: even one heavy outlier can spoil the calculated mean, highlighting the sensitivity of the mean value. Suspected outliers can be excluded by calculating trimmed sample means: the α% trimmed mean excludes α% of the data at the low end and another α% at the high end of the values, 2α% in total. The 50% trimmed mean is the median m. It is the most robust estimator with an asymptotic breakdown point of 1/2. The α% trimmed mean has a breakdown point of α, its trimming fraction, forming a continuum between the sample mean and the sample median with respect to the asymptotic breakdown point.

The accuracy can be expressed as the asymptotic variance σ_θ^2 associated with the estimator. It is generally not equal to the population variance. The efficiency of different estimators can be compared via the ratio of their variances, called asymptotic relative efficiency. ($ARE = \sigma_A^2/\sigma_B^2$, where $\sigma_A^2 \leq \sigma_B^2$, thus $ARE \leq 1$, higher ARE indicating smaller variance when comparing more estimators) However, unlike the breakdown points, the variances of the estimators depend on the underlying distribution type (which is unknown), rendering their comparison difficult. Generally, the more robust an estimator is, the less effective it is, and vice versa.

A comprehensive summary on the breakdown point and relative efficiency is given in [21].

In the following sections, a statistical "toolbox" for making estimations about the 5% fractile, and more importantly, the mean or median value will be presented. The properties of $\bar{x}$

and s_x^2 as unbiased, consistent estimators for μ and σ_x^2 respectively will be put to use.

4.2 Nonparametric estimation of the 5% fractile

When estimating low and/or high fractiles, the shape of the distribution has a strong effect on the outcome. This is especially pronounced for very low probabilities such as failure probabilities, as pointed out by [22]. The influence of the distribution tail shape is important in case of the 5% fractile, too. If the underlying distribution for a dataset is uncertain, one can make use of the following methods and theorems.

$$P\left(|x-\mu| \geq h \cdot \sigma\right) \leq \frac{1}{h^2} \tag{19}$$

Chebyshev's inequality (19) can be used for estimating fractiles, as described in [14]: constructing a two-tailed, 90% confidence interval by setting $P = 0.90$ in (19), $h = \sqrt{1/p}$ and calculating the interval bounds with

$$\bar{x} \pm h \cdot s_x \tag{20}$$

The advantage of this method – besides its simplicity – is that it works for any continuous distribution but with the drawback of providing very wide confidence intervals, i.e. low efficiency. (For $P = 0.90$, $h = 3.162$, compared to $1.645\sqrt{1+1/n}$ in Eq.(2).)

Another easy-to-apply method to estimate the 5% fractile is the method of order, presented in Section 2.1, which works for any continuous distribution, provided enough data points are available. As discussed in Section 3, this requirement is usually fulfilled for CPT data from a single layer. With an increasing number of measurements, the "resolution" around the given fractile is refined too, ensuring its consistency.

The ratio of the method of order 5% fractiles x_k^{mo} to the normal distribution 5% fractiles x_k^{norm} from Eq. (1), as well as to the corresponding lognormal 5% fractiles x_k^{logn} are shown in Fig. 8a and 8b, plotted against the sample skewness γ. Both plots suggest a fairly linear regression curve. The full lines show the linear trend, while the dashed curves delineate the prediction bands for the mean.

As expected, both Fig. 8a and 8b show that the 5% fractiles calculated by the method of order tended to be more and more favourable than the fractiles calculated by Eq. (1) or by the lognormal distribution for increasing positive skewness. Both show an intercept ≈1 (1.05 and 0.93), but in Fig. 8a the coefficient of determination is only R^2 =0.236, while in Fig. 8b it is R^2 =0.578. The negative value appearing in Fig. 8a comes from a negative estimation of x_k^{norm}. Such negative predictions are not possible with the lognormal distribution, but it still fails to address the systematic deviation with the skewness.

This implies that estimating the 5% fractile for CPT cone resistances should be carried out preferably by the method of order, or by applying Eq. (1) to the logarithm of the data, instead of its direct application or the use of Chebyshev's inequality.

4.3 Estimation of the mean and median

As mentioned in Section 4.1, the conflicting issues for selecting an estimator for the "central value" are robustness and efficiency. Robustness was dealt with there, and the efficiency of estimating the mean and median with a given confidence level will be investigated here.

The median m is another robust measure of a "central value" of a distribution, it is defined as $F(m) = 1/2$; the 50% fractile, or alternatively, the 50% trimmed mean. For symmetrical distributions it equals the mean μ, whereas for skewed distributions $\mu \neq m$. (Even in the literature, the mean is sometimes falsely referred to as the 50% fractile.)

Its point estimator is the sample median $\bar{m}$, defined as

$$\bar{m} = \begin{cases} x_{(n+1)/2} & \text{for odd } n \\ \frac{x_{n/2}+x_{n/2+1}}{2} & \text{for even } n \end{cases} \tag{21}$$

The associated hypothesis test is the sign test; it can be used to construct exact nonparametric confidence intervals for the median.

The test statistic

$$\begin{aligned} &T = \sum_{i=1}^{n} I\left(x_i - m\right) \text{ where} \\ &I\left(x_i - m\right) = 1 \text{ if } \mathrm{x_i - m} > 0 \text{ and} \\ &I\left(x_i - m\right) = 0 \text{ if } \mathrm{x_i - m} \leq 0 \end{aligned} \tag{22}$$

follows a binomial distribution with n trials and a success probability of $p = 1/2$:

$$P\left(T \leq k\right) = \sum_{i=0}^{k} \binom{n}{i} p^i \left(1-p\right)^i \tag{23}$$

The n data points divide the real line into $n+1$ intervals; they are also the endpoints of the confidence intervals. After arranging the data points in sorted order ($x_1' \leq \cdots \leq x_n'$), the confidence level for the interval encompassed by endpoints lying "k number of steps inwards" from the outermost data points is

$$1 - 2\,P\left(T \leq k\right) \tag{24}$$

The confidence levels assume discrete values. The 95% confidence level can be approximated as $k_{max}: \; 1 - 2\,P\left(T \leq k_{max}\right) \geq 0.90$; with k_{max} being the largest integer for which the relation holds. (The expression (24) is associated with the two-tailed confidence interval.) [21]

An important advantage of the sign test is that it allows for asymmetric confidence intervals if the dataset is skewed.

For estimating the mean, the central limit theorem can be put to use. It states that the sample mean follows a normal distribution:

$$\bar{x} \sim N\left(\mu, \frac{\sigma_x^2}{n}\right) \tag{25}$$

regardless of the distribution of x. The variance of the estimator $\bar{x}$ is σ_x^2, the population variance, which can be substituted by s_x^2.

Similarly, for large n the sample median also follows a normal distribution (the binomial distribution approaches the normal distribution):

$$\bar{m} \sim N\left(m, \frac{\sigma_m^2}{n}\right) \tag{26}$$

where the variance of the sample median can be calculated from the PDF of the distribution:

$$\sigma_m^2 = \frac{1}{4f(m)^2} \tag{27}$$

Many of the symmetrical distributions are so-called location-scale-type distributions, where the mean is defined by one parameter only and directly. In these cases, the mean can also be estimated via maximum likelihood. The Cramér-Dugué theorem states that the MLEs $\hat{\theta}$ follow a normal distribution with mean at the true value θ, and the variance $I_n\left(\hat{\theta}\right)^{-1}$, the inverse of the Fisher information associated with the distribution. [13]

$$\hat{\theta} \sim N\left(\theta, I_n\left(\hat{\theta}\right)^{-1}\right) \tag{28}$$

The Fisher information can be derived – under some regularity conditions - with the help of the likelihood-function (15). (These regularity conditions can be found e.g. in [13]. For distributions with multiple parameters, the Fisher information becomes a matrix, and the variance of one parameter is the corresponding element in the trace of the inverted Fisher information matrix. [23])

Furthermore, the Cramér-Rao inequality gives a lower bound on the variance of unbiased estimators: it is the inverse of the Fisher information $I_n(\theta)$ [13]. Together with the Cramér-Dugué theorem, it follows that under the regularity conditions for the Fisher information, the MLEs are the most effective estimators.

The variances for σ_x^2, σ_m^2, and for the MLEs of some location parameters are given in Table 3 for comparison of the variances.

For symmetrical, location-scale-type distributions, under the asymptotical normality of both $\bar{x}$, $\bar{m}$ and $\hat{\theta}$, the length of their confidence intervals will be proportional to $1/\sqrt{ARE}$, with $\sigma_{\hat{\theta}}^2 = \sigma_A^2$ (the MLE being the reference estimator). For the normal distribution, this means that $\bar{x}$ has also minimum variance ($ARE = 1$), and the median has a confidence interval $\sim 1,25$ times bigger than the mean. For the logistic distributions, the confidence intervals for $\bar{x}$ and $\bar{m}$ are $\sim 1,05$ and $\sim 1,15$ times wider than for $\hat{\theta}$. These points emphasise the good efficiency of $\bar{x}$.

The lognormal distribution requires special attention: if the estimation of the parameters μ and σ is performed by calculating the sample mean $\mu \approx \bar{x}$ and sample standard deviation $\sigma \approx s_x$ from the logarithm of the observations Y=lnX, then the mean after the back-transformation will be $e^{\mu+\sigma^2/2}$ instead of e^{μ}, which is the median. This is the reason why the lognormal distribution is sometimes criticized for giving too high averages. Furthermore, since the mean, median and location parameter μ are not equal, the comparison of their variances via ARE is pointless (as for the other distributions in Table 3).

To compare the above considerations with the confidence intervals for $\bar{x}$ and $\bar{m}$ based on the current datasets, a nonparametric method called bootstrapping was used to calculate the distribution of both $\bar{x}$ and $\bar{m}$ for each dataset. The bootstrap is essentially a re-sampling plan to create a numerical approximation for any function of the observations (in this case the mean and median), without making assumptions about the underlying distribution type [26]. A bootstrap replication (or bootstrap sample) of the observed data $x_1 \ldots x_n$ is generated by randomly drawing n elements "with replacement" from the dataset. The number of possible combinations with repetition is

$$N = \binom{2n-1}{n} \tag{29}$$

with the actual dataset being one of the possible outcomes (as "drawing n values without replacement"). Even for the shortest dataset analyzed, with $n = 63$, $N > 10^{36}$.

Creating a large number B of replications and subsequently calculating $\bar{x}$ and $\bar{m}$ for each of them enables one to set up an approximation for the distribution of $\bar{x}$ and $\bar{m}$, respectively.

The distribution of $\bar{x}$ was estimated for each of the 125 datasets from $B = 1000$ replications. The results clearly show normal distribution as expected due to the central limit theorem. The maximal difference between the mean of the dataset and the expectation of the bootstrap samples was approximately 0.1%. The latter was calculated as

$$\frac{\left|\bar{x} - \sum_{i=1}^{B} \bar{x}_{B,i}/B\right|}{\bar{x}} \tag{30}$$

with $\bar{x}$ being the mean of the dataset, and $\bar{x}_{B,i}$ being the mean of the i-th bootstrap sample. The greatest difference in the calculated standard deviations – calculated in a similar manner – was approx. 2%. The calculated skewness and kurtosis for each dataset was in the range $\gamma = -0.104$ to 0.304 and $\kappa = 2.88$ to 3.14. Of course, these bounds are subject to slight changes due to the random selection of the B replications out of the possible N, but – given the increasing sensitivity of higher order moments γ and κ against outliers – they nevertheless show that $\bar{x}$ follows a normal distribution as predicted by the central limit theorem.

The procedure was also repeated for $\bar{m}$, but with unsatisfactory results. For $B = 1000$, the anticipated binomial distribution did not emerge in the histograms. An increase to $B = 10000$ resulted in some improvement, but the results were still not satisfying, indicating a slower convergence rate towards the limit in Eq. (23).

Finally, the relative positions of the mean and median $\bar{m}/\bar{x}$, as well as the lengths of their respective 90% confidence intervals $L_{\bar{m}}/L_{\bar{x}}$, and the relative positions of the lower bounds of the intervals m_{low}/x_{low} were compared. Here, $L_{\bar{m}}$ is the length of the confidence interval for $\bar{m}$ as in (21)-(24) and $L_{\bar{x}}$ is the same for $\bar{x}$ as in (7). m_{low} and x_{low} are the lower bounds of $L_{\bar{m}}$ and $L_{\bar{x}}$. The results are shown in Fig. 9a, b, and c respectively.

Tab. 3. Overview of the mean, median, and associated variances of the tested distributions (*: not shown) (γ is the Euler-Mascheroni constant, $\Gamma_R^{-1}()$ is inverse of the regularized incomplete gamma function)

Name	*Parameters*	*Mean*	*Variance*	*Median*	*Variance of median*	I_n^{-1}	*Ref.*
Beta	a, b, α, β	$a + \frac{\alpha}{\alpha+\beta}(b-a)$	$\frac{\alpha\beta}{(\alpha+\beta)^2(1+\alpha+\beta)}$	$a + I_{0.5}^{-1}(\alpha,\beta)(b-a)$	*		
Cauchy	a, b	–	–	a	$\frac{\pi^2 b^2}{4}$		
Extreme Value	α, β	$\alpha + \gamma\beta$	$\frac{\pi^2\beta^2}{6}$	$\alpha - \beta\ln[\ln(2)]$	$\frac{\beta^2}{\ln(2)^2}$		
Gamma	α, β	$\alpha\beta$	$\alpha\beta^2$	$\beta\Gamma_R^{-1}(\alpha, 0, 0.5)$	*		
Gumbel	α, β	$\alpha - \gamma\beta$	$\frac{\pi^2\beta^2}{6}$	$\alpha + \beta\ln[\ln(2)]$	$\frac{\beta^2}{\ln(2)^2}$		
Inverse Gauss	μ, λ	μ	$\frac{\mu^3}{\lambda}$	–	$\frac{\pi\mu^3}{2\lambda}$		
Laplace	μ, β	μ	$2\beta^2$	μ	β^2		
Logistic	μ, β	μ	$\frac{\pi^2\beta^2}{3}$	μ	$4\beta^2$	$\mu : 3\beta^2/n$	[24]
Lognormal	μ, σ	$e^{\mu+\frac{\sigma^2}{2}}$	$(e^{\sigma^2}-1)e^{2\mu+\sigma^2}$	e^{μ}	$\frac{1}{2}e^{2\mu}\pi\sigma^2$	$\mu : e^{2\mu}\sigma^2/n$	[25]
Maxwell	σ	$2\sqrt{\frac{2}{\pi}}\sigma$	$\frac{(3\pi-8)\sigma^2}{\pi}$	$\sigma\sqrt{2\Gamma_R^{-1}(1.5, 0.5)}$	*		
Normal	μ, σ	μ	σ^2	μ	$\frac{\pi\sigma^2}{2}$	$\mu : \sigma^2/n$	[13]
Rayleigh	σ	$\sqrt{\frac{\pi}{2}}\sigma$	$\left(2-\frac{\pi}{2}\right)\sigma^2$	$\sqrt{\ln(4)}\sigma$	$\frac{\sigma^2}{\ln(4)}$		
Weibull	α, β	$\beta\Gamma\left(1+\frac{1}{\alpha}\right)$	$\beta^2[\Gamma(1+\frac{2}{\alpha}) - \Gamma(1+\frac{1}{\alpha})^2]$	$\beta\ln(2)^{\frac{1}{\alpha}}$	*		

As expected, the value of $\bar{m}$ decreases against $\bar{x}$ with increasing skewness. The trend appears to be nearly linear, but some significant downward deviations are present. The lengths $L_{\bar{m}}$ are generally larger than $L_{\bar{x}}$, but no obvious trend is present. However, the larger confidence interval lengths appear in Fig. 9c as a larger scatter of the data. (R^2 =0.322 in Fig. 9c against R^2 =0.535 in 9a, while the regression lines show only slight differences.)

For sample sizes encountered when analyzing CPT data (n >30-50), the bootstrap re-sampling of the datasets has confirmed the statement of the central limit theorem, that $\bar{x}$ is normally distributed with the true (population) mean μ as the expectation. In such a case, the $\bar{x}$ is also the most effective estimator of μ, as seen from Table 3.

Although exact nonparametric confidence intervals can be constructed for m, they were found to be generally larger than those for $\bar{x}$. The difference was even greater than expected from Table 3. The larger robustness of the median was not found to be of particular advantage, since it comes into play in small sample situations or without outlier screening.

Therefore, using Eq. (7) or (8) is appropriate for the calculation of confidence intervals for the mean, regardless of the distribution of the sample.

4.4 Independency of CPT data

An additional consideration should be made when applying these statistical methods to CPT data. The classical statistical methods, be they parametric or nonparametric, share the assumption of independent and identically distributed data. It is a well-known fact that the CPT tip resistances are correlated. For correlated data, methods based on time-series analysis are more appropriate, but that involves very different types of tasks to be solved. A related application of such a random-field analysis to CPT is presented e.g. in [20].

5 Conclusions

The soil properties adopted for geotechnical design have to consider both material-related and testing-related uncertainties. Eurocode 7 defines a statistical principle to select the characteristic values for soil properties: the probability of a more unfavourable value of a parameter should not exceed 5%. Eurocode 7 further notes that the 5% fractile is required if local failure is concerned in the particular limit state; and the spatial mean value at a confidence level of 95% if a larger ground volume is affected. However, it is not clearly stated whether one- or two-tailed confidence intervals should be adopted. Along with the general perception of two-tailed confidence intervals, the above principle is obeyed when setting the confidence level to 90%. In this case, one half of the excluded 10% is favourable (in the upper tail if low values are unfavourable), which leaves 5% probability to more unfavourable values. Most textbooks present statistical formulae based on assuming a normal or lognormal distribution for the quantitative soil property.

The aim of this paper was to investigate the applicability of those formulae for CPT tip resistances. For this end, statistical tests were carried out on 125 datasets from homogeneous soil layers, confirmed by borehole logs. The goodness-of-fit was tested with the Kolmogorov test against 13 distributions, selected to cover a wide range of choices. The parameters for the fitting procedure were calculated as maximum likelihood estimators, being the most effective estimators available.

The raw Kolmogorov test results, as well as their normalized values have shown that the normality assumption clearly does not hold. The 4-parameter beta, logistic, extreme value, and lognormal distributions were found to be the best-fitting ones, and the lognormal seems to be the most suitable for general use,

due to its relative simplicity and its link to the well-understood normal distribution. Tentatively, a goodness-of-fit of 0.35-0.40 by the Kolmogorov test may already be convincing for the fit.

A number of methods were examined for the estimation of the 5% fractile, and the so-called method of order is suggested for use with CPT data. The first reason is that it is a nonparametric method, i.e. no assumption about the distribution type is necessary. Second, the geological formations which are perceived as homogeneous, distinct layers in geotechnical engineering bear enough CPT data to enable a fine resolution of the distribution around the 5% fractile.

The construction of two-tailed confidence intervals for both the mean and median were examined, regarding the robustness of the estimation and its efficiency. The investigations and comparisons have shown that the mean is normally distributed – as stated in the central limit theorem – regardless of the underlying distribution of the data. That enables effective estimation with small errors, especially compared with the confidence intervals around the median. Although the preliminary considerations about the median promised, along with higher robustness, only slightly larger confidence intervals, this was not confirmed by the bootstrap distributions. The latter were found to scatter strongly, and yielding considerably more unfavourable results in most cases.

The main results of this paper may add a simple method for estimating the 5% fractile to the geotechnical engineers' statistical toolbox, and provide verification for the use of the common methods for constructing confidence intervals for the mean value of CPT data. On the other hand, it demonstrates the inappropriateness of assuming a normal distribution for CPT tip resistances in a homogeneous layer.

References

1 **Fellin W**, *Assessment of characteristic shear strength parameters of soil and its implication in geotechnical design*, In: **Fellin W, Lessmann H, Oberguggenberger M, Vieider R** (eds.), Analyzing Uncertainty in Civil Engineering, Springer; Berlin Heidelberg New York, 2005, pp. 1–14.

2 **Baecher GB, Christian JT**, *Reliability and Statistics in Geotechnical Engineering*, Wiley and Sons; Chichester, 2003, ISBN 0471498335.

3 **Bond A., Harris A.**, *Decoding Eurocode 7*, Taylor & Francis; London and New York, 2008, ISBN 9780415409483.

4 **Frank R, Bauduin C, Driscoll R, Kavvadas M, Krebs Ovesen N, Orr L, Schuppener B**, *Designers' Guide to EN 1997-1 Eurocode 7*, Thomas Telford; London, 2004, ISBN 9780727731548.

5 **Gulvanessian H, Calgaro J, Holický M**, *Designers' Guide to EN 1990*, Thomas Telford; London, 2002, ISBN 9780727730114.

6 **Orr T**, *Selection of characteristic values and partial factors in geotechnical designs to Eurocode 7*, Computers and Geotechnics, **26**, (2000), 263–279, DOI 10.1016/S0266-352X(99)00042-7.

7 **Takács A**, *Some statistical aspects of the semi-probabilistic approach (partial factoring) of the Eurocode 7*, Periodica Polytechnica Civil Engineering, **55**, (2011), 45–52, DOI 10.3311/pp.ci.2011-1.06.

8 **Lunne T, Robertson PK., Powell JJM**, *Cone Penetration Testing in Geotechnical Practice*, Blackie Academic & Professional; London, 1997, ISBN 9780419237501.

9 **Fellenius BH**, *The Red Book — Basics of Foundation Design (electronic edition, Dec. 2011)*, 2011, `www.fellenius.net`. last accessed: May 4, 2012.

10 **Mayne PW**, *NCHRP Synthesis 368 — Cone Penetration Testing*, Transportation Research Board; Washington D.C., 2007. ISBN: 9780309097840.

11 **Mahler A**, *The use of cone penetration test in pile design*, Periodica Polytechnica Civil Engineering, **47**(2), (2003), 189–197, DOI 10.3311/pp.ci.2003-2.04.

12 **Pusztai J**, *Suggestion to the Determination of the Bearing Capacity of Piles on the Basis of CPT Sounding Tests*, Periodica Polytechnica Civil Engineering, **48**(1-2), (2004), 39–46, DOI 10.3311/pp.ci.2004-1-2.04.

13 **Bolla M, Krámli A**, *Statisztikai következtetések elmélete (Theory of statistical inference)*, Typotex; Budapest, 2005, ISBN 9789639548411. in Hungarian.

14 **Rétháti L**, *Probabilistic Solutions in Geotechnics*, Elsevier; Amsterdam, 1988, ISBN 9780444989604.

15 **Sia AHI, Dixon N**, *Distribution and variability of interface shear strength and derived parameters*, Geotextiles and Geomembranes, **25**, (2007), 139–154, DOI 10.1016/j.geotexmem.2006.12.003.

16 **D'Agostino RB, Belanger A, D'Agostino RBJ**, *A Suggestion for Using Powerful and Informative Tests of Normality*, The American Statistician, **44**(4), (1990), 316–321.

17 *Wolfram Mathematica Documentation Center, Parametric Statistical Distributions*, Wolfram Research, 2012, `http://reference.wolfram.com/mathematica/guide/ParametricStatisticalDistributions.html`. last accessed: May 4, 2012.

18 **Mahler A**, *Statikus szondázási eredmények hasznosítása (Utilization of CPT test results)*, PhD thesis, Budapest Univ. of Technology and Economics, Dept. of Geotechnics; Budapest, 2007. in Hungarian.

19 **Mendenhall W, Sincich T**, *Statistics for Engineering and the Sciences*, Pearson Prentice Hall; New Jersey, 2007, ISBN 9780131877061.

20 **Phoon KK, Quek AT, An P**, *Identification of Statistically Homogeneous Soil Layers Using Modified Bartlett Statistics*, Journal of Geotechnical and Geoenvironmental Engineering, **129**, (2003), 649–659, DOI 10.1061/(ASCE)1090-0241(2003)129:7(649).

21 **Geyer CJ**, *Stat 5102 Notes — Nonparametric tests and confidence intervals (April 13, 2003)*, 2003, `http://www.stat.umn.edu/geyer/old03/5102/notes/rank.pdf`. last accessed: May 4, 2012.

22 **Oberguggenberger M, Fellin W**, *From Probability to Fuzzy Sets*, In: **Pöttler R, Klapperich H., Schweiger H.** (eds.), Proceedings of the International Conference on Probabilistics in Geotechnics: Technical and Economic Risk Estimation, United Engineering Foundation; New York, 2002, pp. 29–38.

23 **Geyer CJ**, *Stat 5102 Notes — Fisher Information and Confidence Intervals Using Maximum Likelihood (March 7, 2003)*, 2003, `http://www.stat.umn.edu/geyer/old03/5102/notes/fish.pdf`. last accessed: May 4, 2012.

24 **deCani JS, Stine RA**, *A Note on Deriving the Information Matrix for a Logistic Distribution*, The American Statistician, **40**(3), (1986), 220–222, `http://www.jstor.org/stable/2684541`.

25 **Alshunnar FS, Raqab MZ, Kundu D**, *On the comparison of the Fisher information of the log-normal and generalized Rayleigh distribution*, Journal of Applied Statistics, **37**, (2010), 391–404, DOI 10.1080/02664760802698961.

26 **Efron B**, *Nonparametric standard errors and confidence intervals*, The Canadian Journal of Statistics, **9**(2), (1981), 139–158, `http://www.jstor.org/stable/3314608`.

Appendix

Tab. 4. Overview of the analyzed soil layers from the industrial site

CPT profile	**layer**	**starting depth** [m]	**final depth** [m]	**thickness** [m]	**soil type** [borehole, lab.]	**soil type** [Robertson, 1986]	**data points** *n*
HK 1	A	0.72	3.60	2.88	loessy, low pl. **clay** - hard	6	145
	B	3.62	6.34	2.72	loessy, low pl. **clay** - firm	5	133
	C	6.36	14.72	8.36	loessy, low pl. **clay** - soft	3 - 4 - 5	118
	D	14.88	18.88	4.00	loessy, low pl. **clay** - firm	3	148
HK 2	A	0.66	3.30	2.64	loessy, low pl. **clay** - hard	(6) - 7	150
	B	3.32	6.02	2.70	loessy, low pl. **clay** - firm	5 - (6)	191
	C	6.04	18.16	12.12	loessy, low pl. **clay** - soft	(4) - 5	141
	E	18.40	20.56	2.16	loessy, low pl. **clay** - hard	(5) - 11	200
HK 3	A	1.12	3.46	2.34	loessy, low pl. **clay** - hard	6	172
	B	3.48	6.62	3.14	loessy, low pl. **clay** - firm	(4) - 5	198
	C	6.64	16.80	10.16	loessy, low pl. **clay** - soft	3 - (4) - (5)	170
	D	16.82	18.32	1.50	loessy, low pl. **clay** - firm	3	96
HK 4	A	0.82	3.76	2.94	loessy, low pl. **clay** - hard	(6) - 7	137
	B	3.78	8.16	4.38	loessy, low pl. **clay** - firm	(5) - 6	136
	C	8.18	16.32	8.14	loessy, low pl. **clay** - soft	(4) - 5 - (6)	158
	E	16.34	17.40	1.06	loessy, low pl. **clay** - hard	6 - 7 - 9	220
HK 5	A	1.06	4.04	2.98	loessy, low pl. **clay** - hard	6 - (7)	283
	B	4.06	9.70	5.64	loessy, low pl. **clay** - firm	(4) - (5) - 6	286
	C	9.72	16.88	7.16	loessy, low pl. **clay** - soft	(5) - 6	354
	D	18.08	25.68	7.60	loessy, low pl. **clay** - firm	(6) - 11	247
	E	17.00	18.06	1.06	loessy, low pl. **clay** - hard	(3) - 4 - 5	245
HK 6	A	0.92	4.72	3.80	loessy, low pl. **clay** - hard	(5) - 6	281
	B	4.74	10.44	5.70	loessy, low pl. **clay** - firm	(3) - 5 - (6)	309
	C	10.46	17.40	6.94	loessy, low pl. **clay** - soft	(3) - 5	330
HK 7	A	1.50	4.30	2.80	loessy, low pl. **clay** - hard	(6) - 7	419
	B	4.32	11.38	7.06	loessy, low pl. **clay** - firm	(4) - (5) - 6	607
	C	11.40	18.24	6.84	loessy, low pl. **clay** - soft	(4) - 5 - (6)	509
HK 8	A	0.40	4.38	3.98	loessy, low pl. **clay** - hard	7	408
	B	4.40	9.32	4.92	loessy, low pl. **clay** - firm	5 - 6	359
	C	9.34	16.42	7.08	loessy, low pl. **clay** - soft	(4) - 5 - (6)	348
	D	17.74	24.86	7.12	loessy, low pl. **clay** - firm	4 - 5	343
	E	16.52	17.72	1.20	loessy, low pl. **clay** - hard	4 - 5	355
HK 9	A	3.36	6.78	3.42	loessy, low pl. **clay** - hard	6 - 7	414
	B	6.80	11.68	4.88	loessy, low pl. **clay** - firm	(4) - 5 - 6	388
	C	11.72	19.98	8.26	loessy, low pl. **clay** - soft	(4) - 5 - (6)	309
HK 10	A	3.38	7.32	3.94	loessy, low pl. **clay** - hard	(5) - 6	407
	B	7.40	13.00	5.60	loessy, low pl. **clay** - firm	3 - 5	201
	C	13.18	20.92	7.74	loessy, low pl. **clay** - soft	(4) - 5 - (6)	76
HK 11	A	4.20	7.58	3.38	loessy, low pl. **clay** - hard	6 - 7	381
	B	7.60	13.76	6.16	loessy, low pl. **clay** - firm	3 - 4 - 5	357
	C	13.78	19.94	6.16	loessy, low pl. **clay** - soft	5 - (6)	109
HK 12	A	3.10	5.00	1.90	loessy, low pl. **clay** - hard	5 - (6)	54
	B	5.02	11.60	6.58	loessy, low pl. **clay** - firm	3 - 5	54
	C	11.62	19.74	8.12	loessy, low pl. **clay** - soft	3 - 5 - 6	61

Tab. 5. Overview of the analyzed soil layers at the road construction site (* not reached by borehole, clearly homogeneous in CPT)

CPT profile	layer	starting depth [m]	final depth [m]	thickness [m]	soil type [borehole, lab.]	soil type [Robertson, 1986]	data points *n*
1 A	A	1.10	14.70	13.60	clayey **silt**	5 - (6)	656
	B	16.10	20.20	4.10	clayey **silt**	4 - 5 - 6	189
	C	20.30	24.30	4.00	- *	11 - (3)	183
6	A	4.40	9.40	5.00	clayey **silt**	5 - 6 - 7	237
	B	9.42	16.50	7.08	clayey **silt**	3 - (4) - (5)	335
6 K	A	4.82	9.28	4.46	clayey **silt**	5 - 6 - 7	223
	B	9.30	16.66	7.36	clayey **silt**	3 - (4) - (5)	352
8	A	4.94	8.80	3.86	silty **sand** (loess)	6	190
	B	9.24	12.50	3.26	low plast. **clay**	5	154
	C	14.84	18.80	3.96	low plast. **clay**	3 - 5	199
8 K	A	3.76	8.92	5.16	silty **sand** (loess)	6	246
	B	9.08	12.64	3.56	low plast. **clay**	5	168
	C	12.72	17.64	4.92	low plast. **clay**	5	226
12	A	1.70	9.60	7.90	silty **sand**	6 - 7	380
	B	17.78	23.00	5.22	silty **sand**	3 - 6 - 7	235
12 K	A	1.86	9.30	7.44	silty **sand**	6 - 7	355
	B	16.40	22.94	6.54	silty **sand**	3 - 6 - 7	298
15	A	1.06	5.60	4.54	silty **sand**	5 - 6 - 7	222
	B	6.10	9.64	3.54	silty **sand**	7	171
15 K	A	0.80	5.66	4.86	silty **sand**	5 - 6 - 7	235
	B	6.10	9.20	3.10	silty **sand**	7	149
16	A	1.32	6.80	5.48	medium grained **sand**	8	268
	B	7.10	12.44	5.34	silty **sand**	5 - 6	254
	C	17.62	19.80	2.18	low plast. **clay**	6	107
18	A	3.04	5.60	2.56	silty **sand**	6 - 7 - 8	124
	B	6.54	8.80	2.26	silty **sand**	7	104
18 K	A	3.20	5.60	2.40	silty **sand**	8 - 9	115
	B	6.40	8.68	2.28	silty **sand**	(5) - 6 - 7 - (8)	111
19	A	1.80	6.40	4.60	silty **sand**	3 - 4 - 7	223
	B	14.00	18.14	4.14	medium plast. **clay**	6	192
19 K	A	1.30	6.40	5.10	silty **sand**	3 - 4 - 5	242
	B	14.80	19.68	4.88	medium plast. **clay**	5 - 6	234
20 K	A	9.06	18.40	9.34	silty **sand**	7	445
23	A	5.40	18.70	13.30	sandy **silt**	(7) - 8	642
	B	17.78	21.40	3.62	sandy **silt**	8	128
	C	25.42	29.72	4.30	sandy, silty **clay**	6	209
23 K	A	10.00	13.10	3.10	silty **sand**	6 - (7)	151
	B	13.12	16.00	2.88	silty **sand**	7	139
30	A	2.02	9.36	7.34	silty **sand**	7 - 8	352
	B	11.96	16.76	4.80	silty **clay**	6	232
31	A	6.50	10.00	3.50	**sand** (w. organic bands)	3 - 5	165
	B	18.82	21.86	3.04	- *	6	147
31 K	A	6.60	8.68	2.08	**sand** (w. organic bands)	5 - 6 - 7	100
	B	9.20	11.62	2.42	**sand** (w. organic bands)	5 - 6	120
	C	11.74	13.38	1.64	silty **clay** (w. organic stains)	7	81
485 - 1	A	0.80	2.20	1.40	clayey **silt**	3 - 5	68
	B	2.22	5.60	3.38	silty **sand**	5 - 6 - 7	159
	C	5.62	12.68	7.06	silty **sand**	6 - 7 - 8	334
	D	12.76	18.50	5.74	silty **sand**	8 - 9	265
485 - 2	A	0.80	2.20	1.40	clayey **silt**	3 - 5	69
	B	2.22	5.60	3.38	silty **sand**	5 - 6 - 7	163
	C	5.62	12.68	7.06	silty **sand**	6 - 7 - 8	337
	D	12.76	19.68	6.92	silty **sand**	8 - 9	330
D0	A	4.00	10.50	6.50	silty **sand**	5 - 6	631
	B	16.90	22.39	5.49	silty **sand**	(5-6-7-8-11-12)	535
	C	22.40	29.94	7.54	silty **sand**	(7) - 11 - (12)	677
D1	A	4.00	10.00	6.00	silty **sand**	7 - 8	287
	B	16.90	21.98	5.08	silty **sand**	7 - 8	247
	C	22.00	29.64	7.64	silty **sand**	6 - 7 - 8 - 11	378
D2	A	3.20	4.64	1.44	organic **silt**	2 - 3	73
	B	8.70	16.64	7.94	silty **sand**	7 - 8 - 9	382
	C	20.94	24.98	4.04	silty **sand**	8 - 9	191
D3	A	3.34	4.66	1.32	organic **silt**	2 - 3	64
	B	20.38	25.40	5.02	silty **sand**	3 - 4 - (5)	240
D4 P	A	5.90	8.10	2.20	medium plast. **clay**	3	213
	B	12.40	17.48	5.08	low plast. **clay**	3 - 11	490
	C	18.40	23.20	4.80	medium plast. **clay**	3	463
D4	A	5.90	8.10	2.20	medium plast. **clay**	4	104
	B	12.40	15.00	2.60	low plast. **clay**	3	124
	C	16.10	17.42	1.32	low plast. **clay**	3	63
	D	18.40	23.40	5.00	medium plast. **clay**	5	235
D5	A	4.20	6.12	1.92	medium plast. **clay**	5 - 6	183
	B	6.70	10.56	3.86	medium plast. **clay**	3	378
	C	11.91	14.87	2.96	clayey **silt**	3	288
	D	18.75	22.00	3.25	silty **sand**	4 - 5	305
	E	22.01	25.60	3.59	- *	3 - 5	351
KM - 41	A	4.00	7.00	3.00	sandy, clayey **silt**	6 - 7	143
	B	8.00	15.18	7.18	sandy, clayey **silt**	7	348
KM - 42	A	4.00	7.00	3.00	sandy, clayey **silt**	7	144
	B	8.00	15.18	7.18	sandy, clayey **silt**	7	346
KM - 101	A	6.50	12.20	5.70	silty **sand**	7	275